Suryasentana, S. K. *et al.* (2020). *Géotechnique* **70**, No. 4, 343–353 [https://doi.org/10.1680/jgeot.18.P.251]

A systematic framework for formulating convex failure envelopes in multiple loading dimensions

STEPHEN K. SURYASENTANA*, HARVEY J. BURD†, BYRON W. BYRNE† and AVI SHONBERG‡

The failure envelope approach is widely used to assess the ultimate capacity of shallow foundations for combined loading, and to develop foundation macro-element models. Failure envelopes are typically determined by fitting appropriate functions to a set of discrete failure load data, determined either experimentally or numerically. However, current procedures to formulate failure envelopes tend to be ad hoc, and the resulting failure envelopes may not have the desirable features of being convex and well-behaved for the entire domain of interest. This paper describes a new systematic framework to determine failure envelopes – based on the use of sum of squares convex polynomials – that are guaranteed to be convex and well-behaved. The framework is demonstrated by applying it to three data sets for failure load combinations (vertical load, horizontal load and moment) for shallow foundations on clay. An example foundation macro-element model based on the proposed framework is also described.

KEYWORDS: bearing capacity; failure; footings/foundations; numerical modelling; offshore engineering; soil/structure interaction

INTRODUCTION

Existing failure envelope formulations

The failure envelope approach is widely used to assess the ultimate capacity of shallow foundations for combined loading. There are numerous advantages of this approach compared to classical bearing capacity methods (Terzaghi, 1943; Meyerhof, 1951; Vesić, 1973), as has been discussed extensively in previous work (e.g. Tan, 1990; Gottardi & Butterfield, 1993; Bransby & Randolph, 1998; Martin & Houlsby, 2000; Houlsby & Byrne, 2001). Failure envelopes can also be used to develop plasticity-based macro-element models for shallow foundations (e.g. Nova & Montrasio, 1991; Cassidy, 1999; Martin & Houlsby, 2001; Bienen *et al.*, 2006).

A failure envelope for a specific shallow foundation concept can be determined by measuring, or computing, a set of discrete failure load combinations for different loading conditions (e.g. the experimental data reported in Martin & Houlsby (2000) and the numerical data in Taiebat & Carter (2000)). These failure envelope data are then approximated using an appropriate mathematical formulation (referred to in this paper as a 'failure envelope formulation') together with an optimisation process to achieve a best fit.

In the current paper, V, H and M refer to the applied vertical and horizontal loads, and moment, respectively. Furthermore, $\tilde{H} = H/H_0$, $\tilde{M} = M/M_0$ and $\tilde{V} = V/V_0$ refer to the normalised loads, where H_0, M_0, V_0 are the respective uniaxial capacities. (Uniaxial capacity refers to the failure load for one load component when all other load components are maintained at zero throughout the loading.) In the notation employed in this paper, vectors are denoted in bold face, italic, lower case (e.g. $\boldsymbol{x}$) and matrices are denoted in bold face, upper case, upright font (e.g. $\mathbf{A}$).

Current failure envelope formulations can generally be categorised into one of two groups (although the wide-ranging literature in this area also includes a number of formulations that do not fit into either group, e.g. Taiebat & Carter (2000)). One group represents the failure envelope using a sum of power functions of the applied loads. This approach has been used to represent the 'cigar-shaped' failure envelopes determined from experimental data for shallow foundations on sand (Nova & Montrasio, 1991; Gottardi & Butterfield, 1993; Cassidy, 1999; Gottardi *et al.*, 1999; Byrne & Houlsby, 2001; Bienen *et al.*, 2006) and clay (Martin & Houlsby, 2000). Published formulations of this type are mainly defined for planar VHM loading, although extensions to six degrees-of-freedom loading have been described by Martin (1994), Byrne & Houlsby (2005) and Bienen *et al.* (2006). An example of a formulation in this group is 'Model A' (Martin, 1994), which was developed to represent the failure envelope for a spudcan foundation in clay. Model A is defined as

$$f(\tilde{H}, \tilde{M}, \tilde{V}) = \tilde{H}^2 + \tilde{M}^2 - 16\tilde{V}^2(1 - \tilde{V})^2 = 0 \qquad (1)$$

although for numerical implementation, Martin & Houlsby (2001) recommend the alternative form

$$f(\tilde{H}, \tilde{M}, \tilde{V}) = (\tilde{H}^2 + \tilde{M}^2)^{1/2} - 4\tilde{V}(1 - \tilde{V}) = 0 \qquad (2)$$

The second group of failure envelope formulations, termed 'HM-based', has primarily been used in connection with numerically determined failure envelope data (Feng *et al.*, 2014; Vulpe *et al.*, 2014; Vulpe, 2015; Shen *et al.*, 2016, 2017). Formulations in this group are defined in terms of composite horizontal and moment loads, where the composition provides a means of incorporating the influence of additional load components within a basic HM framework. An example of a formulation in this group (from

Manuscript received 30 October 2018; revised manuscript accepted 28 March 2019. Published online ahead of print 30 April 2019.
Discussion on this paper closes on 1 August 2020, for further details see p. ii.

* Department of Engineering Science, University of Oxford, Oxford, UK (Orcid:0000-0001-5460-5089).
† Department of Engineering Science, University of Oxford, Oxford, UK.
‡ Ørsted Wind Power, London, UK.

Vulpe *et al*. (2014)) is

$$f(\tilde{H}^*, \tilde{M}^*) = \left|\tilde{H}^*\right|^a + \tilde{M}^{*\alpha} + 2b\tilde{H}^*\tilde{M}^* - 1 = 0 \quad (3)$$

where $\tilde{H}^*$ and $\tilde{M}^*$ are composite horizontal and moment loads defined by $\tilde{H}^* = \tilde{H}/(1 - \tilde{V}^{4\cdot69})$ and $\tilde{M}^* = \tilde{M}/(1 - \tilde{V}^{2\cdot12})$; and a and b are parameters ($a = 2\cdot13$ and $b = -0\cdot09$ for $\tilde{V} \leq 0\cdot5$, or $a = 1\cdot63$ and $b = -0\cdot05$ for $\tilde{V} > 0\cdot5$).

Formulation of foundation macro-element models

Failure envelope formulations are a convenient basis for the development of plasticity-based macro-element models for foundations. For example, based on experimental data, Martin & Houlsby (2000) develop a modified version of Model A (termed 'Model B', described further in the later subsection within 'Example applications' entitled 'Model B') as the yield function for a macro-element model of a spudcan foundation in clay.

A macro-element model typically incorporates a yield function and a plastic potential function; these functions govern the admissible load states and the plastic displacements, respectively. The yield function may also contain a hardening parameter that governs the evolution of the yield surface (see Appendix for discussion on the distinction between a yield surface and a yield function). However, the current paper is concerned mainly with developing failure envelope formulations to provide an approximate fit to discrete failure load data. For simplicity, for the macro-element formulation described later in this paper, associated flow (i.e. where the yield function is also the plastic potential function) and perfect plasticity (i.e. no hardening) are adopted.

The yield function adopted in macro-element models should ideally be convex throughout the domain and it is insufficient to have convexity at just the admissible loads boundary (i.e. a convex yield surface). Franchi *et al*. (1990) has discussed the key differences between the yield function and the yield surface and the theoretical relevance of the convexity of the yield function. A summary of the characteristics of convex functions and the difference between a yield surface and a yield function is given in the Appendix. The importance of convexity of the yield function has been largely overlooked, especially in geotechnics, over the past few decades. This particular issue was raised by Panteghini & Lagioia (2014, 2018a, 2018b), who reported numerical problems (e.g. lack of convergence in boundary value problems) when using implicit integration algorithms with non-convex yield functions. To avoid such problems, they propose an approach for providing convexity to the yield functions. For rate-independent, non-hardening/softening materials, a convex yield function has the added benefit of thermodynamic consistency, provided that an associated flow rule is adopted and the yield surface contains the origin of the load space (Ottosen & Ristinmaa, 2005).

Yield (and plastic potential) functions employed in macro-element models must be continuous and real-valued. Ideally, they should also be differentiable with a continuous gradient and Hessian throughout the load domain. Furthermore, they should not have a restricted domain, as it is not known a priori the load states at which implicit integration algorithms will require the evaluation of the yield function. Also, functions should be avoided that have singularities (either in the function itself or its derivatives) at certain load states. For the purposes of the current paper, a function with these ideal attributes is referred to as 'well-behaved'. It is noted that successful plasticity models can be developed on the basis of yield functions that are not well-behaved; the conventional Mohr–Coulomb yield function, for example, provides a common basis for soil constitutive models despite not being differentiable at the 'edges' of the yield surface (although rounding approximations (e.g. Sloan & Booker, 1986) can be employed to address the numerical difficulties associated with these edges). In general, employing non-well-behaved functions is inconvenient from a numerical implementation perspective.

Failure envelope formulations can be used in two separate types of practical application: (*a*) assessment of ultimate foundation capacity and (*b*) representing the yield surface (and the plastic potential for associated flow) in macro-element models. Failure envelope formulations that are suitable for both purposes are therefore particularly convenient. However, not all of the current failure envelope formulations are applicable to both applications, either due to lack of convexity or because they are not well-behaved. For example, the extensive use of fractional exponents for the *HM*-based formulations means that the yield function may not be real-valued in parts of the domain (e.g. equation (3) is not real-valued for $\tilde{M} < 0$ or $\tilde{V} < 0$, since raising negative numbers by fractional powers results in complex values). Furthermore, the composition approach within this group of formulations results in singularities in the function and its gradient at $\tilde{V} = 1$, which makes this form of failure envelope inconvenient for macro-element model implementation. It is noted that the *HM*-based formulations were not developed with macro-element modelling in mind, and thus suitability for this use should not necessarily be expected. However, failure envelopes developed using the formulation framework described in the current paper are guaranteed to be convex and well-behaved; they are therefore applicable to a range of practical applications.

A new framework for convex, well-behaved, failure envelopes

For the purposes of the current paper, a 'globally convex' function is defined as a function that is convex throughout the domain $\mathbb{R}^n$ (real coordinate space of n dimensions, where n is interpreted in the context of the current work as the number of individual load and moment components applied to the foundation). A new framework is proposed for the formulation of failure envelopes that are guaranteed to be globally convex and well-behaved for all possible failure load combinations. Furthermore, the framework is systematic and general. This is significant, as previous researchers (e.g. Gourvenec, 2007) have suggested that difficulties in deriving closed-form expressions to approximate failure envelopes present a practical obstacle to the adoption of the failure envelope approach in design. The proposed framework provides a systematic process that can be applied to failure envelope data sets consisting of multiple load (and moment) components. The framework is also able to represent various failure envelope shapes that correspond to different types of shallow foundation. It therefore facilitates the further development of the failure envelope approach for practical applications.

In developing this framework, it is recognised that proving convexity for a general function is typically a difficult task. For example, a twice differentiable function with a positive semi-definite Hessian throughout its domain is guaranteed to be convex. However, a heuristic approach that demonstrates that a Hessian is positive semi-definite at a finite number of points is insufficient to prove convexity for the entire domain. Conversely, demonstrating non-convexity is often relatively straightforward; a single case where the Hessian is not positive semi-definite is sufficient.

The approach employed in the current framework is therefore to restrict the search for failure envelope formulations to well-behaved polynomial functions that are known a priori to be globally convex. In developing this procedure, use is made of a mathematical technique known as 'sum of squares' (SOS) programming, which provides a computationally tractable method for determining globally convex polynomials.

POLYNOMIAL FAILURE ENVELOPE FORMULATIONS

General homogeneous polynomials

Ellipsoids are a class of well-behaved functions that are guaranteed to be convex, as outlined below. A general ellipsoid can be expressed in the quadratic form

$$f(\boldsymbol{x}) = (\boldsymbol{x}-\boldsymbol{c})^{\mathrm{T}}\mathbf{A}(\boldsymbol{x}-\boldsymbol{c}) = 1 \tag{4}$$

where $\boldsymbol{x}$, $\boldsymbol{c} \in \mathbb{R}^{\mathrm{n}}$ are vectors and $\mathbf{A}$ is a positive definite square constant matrix. The Hessian in this case is $\nabla^2 f(\boldsymbol{x}) = 2\mathbf{A}$ and therefore guaranteed to be positive definite. Since positive definite matrices are also positive semi-definite, it follows that ellipsoids are convex. As ellipsoids are also well-behaved, they are candidates for representing failure envelopes, for which the components of $\boldsymbol{x}$ are the foundation loads (in an appropriate normalised form) and the components of $\mathbf{A}$ and $\boldsymbol{c}$ are selected to provide a best fit with the available failure load data. However, ellipsoids have the significant disadvantage in this application that they are not expressive enough to represent the varied shapes of failure envelopes that correspond to the range of plausible shallow foundation configurations.

Ellipsoids are second degree polynomials; higher degree polynomials provide options for developing failure envelope functions with increased expressiveness. Since polynomials of odd degree ≥ 3 are guaranteed to be non-convex (Ahmadi *et al*., 2013), odd polynomials are excluded as candidates for the current application. Polynomials of even degree ≥ 4 can either be convex or non-convex, but it is typically computationally difficult to prove their convexity in the general case (Ahmadi *et al*., 2013). Thus, this paper considers a subset of polynomials of even degree ≥ 2, called sum of squares convex (SOS-convex) polynomials, for which convexity can be demonstrated in a computationally tractable manner.

Sum of squares polynomials

A polynomial $s(\boldsymbol{x})$ of degree $2d$ (where d is a positive integer) is an SOS polynomial if it can be represented as

$$s(\boldsymbol{x}) = \sum_{j=1}^{n\mathrm{poly}} g_j(\boldsymbol{x})^2 \tag{5}$$

where $g_j(\boldsymbol{x})$ are polynomials of degree $\leqslant d$ and $n$poly is the number of individual polynomials, $g_j(\boldsymbol{x})$, employed in the summation. Equivalently, $s(\boldsymbol{x})$ is SOS if and only if it can be represented as $s(\boldsymbol{x}) = \boldsymbol{z}^{\mathrm{T}}\mathbf{B}\boldsymbol{z}$ where $\mathbf{B}$ is a positive semi-definite matrix and $\boldsymbol{z}$ is a vector of all monomials of degree up to and including d. This can be shown by noting that $s(\boldsymbol{x}) = \boldsymbol{z}^{\mathrm{T}}\mathbf{B}\boldsymbol{z} = \boldsymbol{z}^{\mathrm{T}}\mathbf{Q}^{\mathrm{T}}\mathbf{Q}\boldsymbol{z} = (\mathbf{Q}\boldsymbol{z})^{\mathrm{T}}(\mathbf{Q}\boldsymbol{z}) = \boldsymbol{g}^{\mathrm{T}}\boldsymbol{g}$ (where $\boldsymbol{g}^{\mathrm{T}}\boldsymbol{g}$ is equation (5) and $\mathbf{Q}^{\mathrm{T}}\mathbf{Q}$ is the Cholesky decomposition of $\mathbf{B}$). It is evident from equation (5) that $s(\boldsymbol{x}) \geq 0$ for $\boldsymbol{x} \in \mathbb{R}^n$.

A necessary and sufficient condition for a twice differentiable polynomial $f(\boldsymbol{x})$ to be convex is for its Hessian $\nabla^2 f(\boldsymbol{x})$ to be positive semi-definite (see Appendix). This requires that

$$\boldsymbol{y}^{\mathrm{T}}\nabla^2 f(\boldsymbol{x})\boldsymbol{y} \geq 0 \text{ for all } \boldsymbol{x}, \boldsymbol{y} \in \text{domain of } f \tag{6}$$

A subset of polynomials that satisfy equation (6) is defined by the restricted but more tractable condition

$$\boldsymbol{y}^{\mathrm{T}}\nabla^2 f(\boldsymbol{x})\boldsymbol{y} \text{ is SOS for all } \boldsymbol{x}, \boldsymbol{y} \in \text{domain of } f \tag{7}$$

Polynomials $f(\boldsymbol{x})$ that satisfy equation (7) are convex (although convex polynomials exist that do not satisfy equation (7)). The subset of convex polynomials that satisfy equation (7) is referred to as 'SOS-convex' polynomials (Ahmadi & Parrilo, 2012).

A key benefit of employing SOS-convex polynomials for failure envelope applications is that the requirement in equation (7) can readily be incorporated within the search process for failure envelope formulations using semi-definite programming (Parrilo, 2003). Additionally, SOS-convex polynomials are well-behaved and support general n-dimensional loading. Thus, SOS-convex polynomials form the basis of the failure envelope formulations in the proposed framework.

DETERMINATION OF SOS-CONVEX POLYNOMIAL FAILURE ENVELOPES

Procedures to determine SOS-convex polynomials to provide a fit with failure load data sets are outlined below.

Standardise the data

Failure envelope data typically consist of sets of discrete failure load combinations. These failure load combinations are standardised by

$$\bar{x}_i = \frac{x_i - x_{i,\mathrm{c}}}{x_{i,\mathrm{ref}}} \tag{8}$$

where x_i is a load component, $x_{i,\mathrm{ref}}$ is a reference load and $x_{i,\mathrm{c}}$ is a shift parameter. The purpose of equation (8) is to shift and scale the data such that the values of $\bar{x}_i$ for uniaxial loading in the positive and negative directions (according to the selected coordinate system) are 1 and -1, respectively. Geometrically, this ensures that the failure envelope intersects each $\bar{x}_i$ axis at ± 1. Importantly, if $f(\bar{\boldsymbol{x}})$ is convex, then convexity in $f(\boldsymbol{x})$ is preserved as the mapping in equation (8) is affine (Boyd & Vandenberghe, 2004).

Define the failure envelope functional form

SOS-convex polynomial functions of the standardised loading variables $\bar{\boldsymbol{x}}$, of even degree $2d$ where d is a positive integer, are now sought to represent the failure envelope $f(\bar{\boldsymbol{x}})$. Although SOS-convex polynomials are in general non-homogeneous, homogeneous forms are adopted in the current framework as they have the important advantage that the coefficients for uniaxial loading can be identified straightforwardly, as indicated in step 3 below.

As an example, a homogeneous polynomial $f(\bar{\boldsymbol{x}})$ with degree $2d = 4$ and number of loading dimensions $n = 2$, with coefficients a_i (that are subsequently determined to ensure that the polynomial is SOS-convex) is

$$\begin{aligned} f(\bar{\boldsymbol{x}}) &= f(\bar{x}_1, \bar{x}_2) \\ &= \bar{x}_1^4 a_1 + \bar{x}_1^3 x_2 a_2 + \bar{x}_1^2 \bar{x}_2^2 a_3 + \bar{x}_1 \bar{x}_2^3 a_4 + \bar{x}_2^4 a_5 \end{aligned} \tag{9}$$

The failure envelope is defined by $f(\bar{\boldsymbol{x}}) - 1 = 0$.

Apply the uniaxial conditions

The standardisation process in step 1 requires that the coefficients of all monomials comprising a single loading

variable are 1. (This is to represent failure correctly for uniaxial loading conditions.) For the example in equation (9), this condition gives $a_1 = 1$ and $a_5 = 1$.

Apply symmetry principles

Other coefficients can be determined by exploiting any available symmetry conditions. For the example in equation (9), if the problem is symmetric such that $f(\bar{x}_1, \bar{x}_2) = f(-\bar{x}_1, \bar{x}_2)$, then the coefficients of all monomials that are odd in $\bar{x}_1$ must be zero; in the current example this implies $a_2 = 0$ and $a_4 = 0$.

Set up a convex optimisation problem

To identify the remaining unknown coefficients (there is only one unknown a_3 in the current example but a greater number of coefficients will typically need to be determined at this stage), a convex optimisation problem is set up. This is based on the conditions: (*a*) $f(\bar{\boldsymbol{x}})$ is SOS-convex and (*b*) $f(\bar{\boldsymbol{x}})$ provides a best fit with the failure envelope data by minimising the objective function C

$$C = \sum_{i=1}^{n\text{data}} \left(f\left(\bar{\boldsymbol{x}}_i^{\text{data}}\right) - 1 \right)^2 \tag{10}$$

where $\bar{\boldsymbol{x}}_i^{\text{data}}$ is a set of failure load combinations and $n$data is the size of the data set. The optimisation problem is therefore

$$\begin{aligned} &\text{minimise } C \\ &\text{subject to } \bar{\boldsymbol{y}}^{\mathrm{T}} \nabla^2 f(\bar{\boldsymbol{x}}) \bar{\boldsymbol{y}} \text{ is SOS for all } \bar{\boldsymbol{x}},\ \bar{\boldsymbol{y}} \in \text{domain of } f(\bar{\boldsymbol{x}}) \end{aligned} \tag{11}$$

To solve the SOS program defined in equation (11), it must first be converted into an equivalent semi-definite program. In the current work, the Matlab toolbox 'YALMIP' (Löfberg, 2004) was used to convert SOS problems such as equation (11) automatically to their equivalent semi-definite programs (Löfberg, 2009). Thereafter, the unknown coefficients in $f(\bar{\boldsymbol{x}})$ can be readily determined using this toolbox.

EXAMPLE APPLICATIONS

Three examples are provided below to demonstrate the application of the proposed formulation framework. The first example concerns the failure envelope for a surface circular footing on homogeneous clay; the second example is the failure envelope for a suction caisson foundation embedded in homogeneous clay; the last example is a new failure envelope formulation to represent Model B, which demonstrates that an existing failure envelope formulation can be approximated within the proposed framework to achieve the advantages of global convexity and well-behaved function attributes.

In all the examples, YALMIP was used, in conjunction with the SeDuMi semi-definite solver (Sturm, 1999), to solve the SOS programs. All the failure envelopes for the examples are plotted in the normalised load space (e.g. $\tilde{H}\tilde{M}$). This enables convenient comparison with figures in previous publications (for the case of Model B).

Surface and caisson foundations

The first two examples use the *VHM* failure load combinations for surface and caisson foundations in homogeneous clay, determined as described in Suryasentana *et al.* (2019) using the 'sequential swipe test' in three-dimensional (3D) finite-element analysis. The soil in these cases was modelled as a linear elastic–perfectly plastic von Mises material. Fig. 1 shows the foundation configurations being considered, including the assumed location of the loading reference point (LRP) (which is needed to provide a datum for the definition of the applied moment).

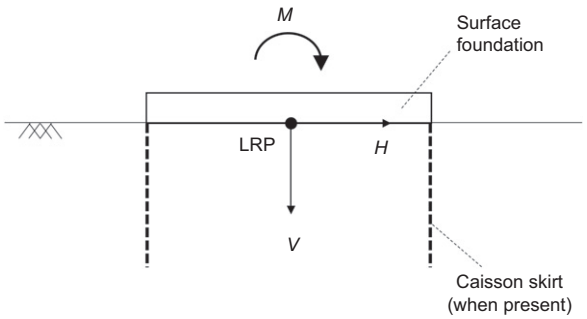

Fig. 1. *VHM* loading configuration for surface foundation and caisson

Based on the numerical failure load data, standardised forms of the failure load data $[\bar{H}, \bar{M}, \bar{V}]$ are obtained, from equation (8), with the computed uniaxial capacities $[H_0, M_0, V_0]$ adopted as the reference values and $[H_c, M_c, V_c] = [0, 0, 0]$ as the shift parameters. The foundations analysed in Suryasentana *et al.* (2019) assumed that the soil and foundation were fully bonded (i.e. no contact breaking) and thus, the foundation has the same tension and compression vertical uniaxial capacities, resulting in $V_c = 0$ in the current example.

Two separate SOS-convex polynomial failure envelopes have been determined: f_4 (with degree $2d = 4$) and f_6 (with degree $2d = 6$). The general forms of these polynomials are

$$\begin{aligned} f_4(\bar{H}, \bar{M}, \bar{V}) = {} & a_1\bar{H}^4 + a_2\bar{H}^3\bar{M} + a_3\bar{H}^2\bar{M}^2 + a_4\bar{H}\bar{M}^3 \\ & + a_5\bar{M}^4 + a_6\bar{H}^3\bar{V} + a_7\bar{H}^2\bar{M}\bar{V} \\ & + a_8\bar{H}\bar{M}^2\bar{V} + a_9\bar{M}^3\bar{V} + a_{10}\bar{H}^2\bar{V}^2 \\ & + a_{11}\bar{H}\bar{M}\bar{V}^2 + a_{12}\bar{M}^2\bar{V}^2 \\ & + a_{13}\bar{H}\bar{V}^3 + a_{14}\bar{M}\bar{V}^3 + a_{15}\bar{V}^4 \end{aligned} \tag{12}$$

$$\begin{aligned} f_6(\bar{H}, \bar{M}, \bar{V}) = {} & a_1\bar{H}^6 + a_2\bar{H}^5\bar{M} + a_3\bar{H}^4\bar{M}^2 \\ & + a_4\bar{H}^3\bar{M}^3 + a_5\bar{H}^2\bar{M}^4 + a_6\bar{H}\bar{M}^5 \\ & + a_7\bar{M}^6 + a_8\bar{H}^5\bar{V} + a_9\bar{H}^4\bar{M}\bar{V} \\ & + a_{10}\bar{H}^3\bar{M}^2\bar{V} + a_{11}\bar{H}^2\bar{M}^3\bar{V} \\ & + a_{12}\bar{H}\bar{M}^4\bar{V} + a_{13}\bar{M}^5\bar{V} + a_{14}\bar{H}^4\bar{V}^2 \\ & + a_{15}\bar{H}^3\bar{M}\bar{V}^2 + a_{16}\bar{H}^2\bar{M}^2\bar{V}^2 \\ & + a_{17}\bar{H}\bar{M}^3\bar{V}^2 + a_{18}\bar{M}^4\bar{V}^2 + a_{19}\bar{H}^3\bar{V}^3 \\ & + a_{20}\bar{H}^2\bar{M}\bar{V}^3 + a_{21}\bar{H}\bar{M}^2\bar{V}^3 + a_{22}\bar{M}^3\bar{V}^3 \\ & + a_{23}\bar{H}^2\bar{V}^4 + a_{24}\bar{H}\bar{M}\bar{V}^4 + a_{25}\bar{M}^2\bar{V}^4 \\ & + a_{26}\bar{H}\bar{V}^5 + a_{27}\bar{M}\bar{V}^5 + a_{28}\bar{V}^6 \end{aligned} \tag{13}$$

Application of the uniaxial condition gives $a_1, a_5, a_{15} = 1$ in f_4 and $a_1, a_7, a_{28} = 1$ in f_6. Additionally, symmetry in $\bar{H}$ and $\bar{M}$ requires that $a_6, a_7, a_8, a_9, a_{13}, a_{14} = 0$ in f_4 and $a_8, a_9, a_{10}, a_{11}, a_{12}, a_{13}, a_{19}, a_{20}, a_{21}, a_{22}, a_{26}, a_{27} = 0$ in f_6. The remaining coefficients are determined from the optimisation in equation (11).

Results. The coefficients for f_4 and f_6 determined from this process are listed in Tables 1 and 2, respectively. Figs 2 and 3 compare the normalised *VH*, *VM* and *HM* failure envelopes determined by $f_4 - 1 = 0$ and $f_6 - 1 = 0$ for the surface and caisson foundation, respectively; also shown are the corresponding 3D finite-element results from Suryasentana *et al.* (2019). Differences between f_4 and f_6 can be seen more clearly in Fig. 4 (which omits the finite-element results).

Both f_4 and f_6 are seen to provide reasonably good approximations of the computed data, although there is a small under-prediction of the *VM* failure envelope for the suction caisson (Fig. 3(b)) and f_4 is unconservative compared to f_6 for the surface foundation at high vertical loads (Fig. 2(c)). It is seen that f_6 provides a better fit with the numerical data than f_4 for the surface foundation (Fig. 2(c)), but f_4 is marginally better for the caisson (Fig. 3(c)). This is confirmed by the data in Table 3, which shows values of the objective function (and their root-mean) at the end of the optimisation process (the smaller the better).

Table 1. Best-fit coefficients in f_4 for the failure envelope data from Suryasentana *et al.* (2019)

Foundation	a_2	a_3	a_4	a_{10}	a_{11}	a_{12}
Surface	−0·36	0·9	−1·43	0·4	0·84	1·64
Caisson	3·55	5·12	3·51	1·72	3·59	2·07

Model B

Model A, introduced in the earlier section 'Existing failure envelope formulations', is representative of a class of functions used by numerous authors to represent yield envelopes. A modified form of this model termed 'Model B', found to provide an improved fit to experimental data of spudcan performance on clay, is described in Martin (1994) and Martin & Houlsby (2000). The Model B formulation is

$$f(\tilde{H}, \tilde{M}, \tilde{V}) = \tilde{H}^2 + \tilde{M}^2 - 2e\tilde{H}\tilde{M} - \beta^2 \tilde{V}^{2\beta_1}(1 - \tilde{V})^{2\beta_2} = 0 \quad (14)$$

Table 2. Best-fit coefficients in f_6 for the failure envelope data from Suryasentana *et al.* (2019)

Foundation	a_2	a_3	a_4	a_5	a_6	a_{14}	a_{15}	a_{16}	a_{17}	a_{18}	a_{23}	a_{24}	a_{25}
Surface	−0·33	1·22	−2·17	2·34	−1·86	0·03	0·34	1·1	0·29	0·84	1·97	1·52	4·72
Caisson	5·18	11·9	15·45	11·96	5·2	2·72	10·86	17·27	13·23	4·21	2·13	2·93	1·04

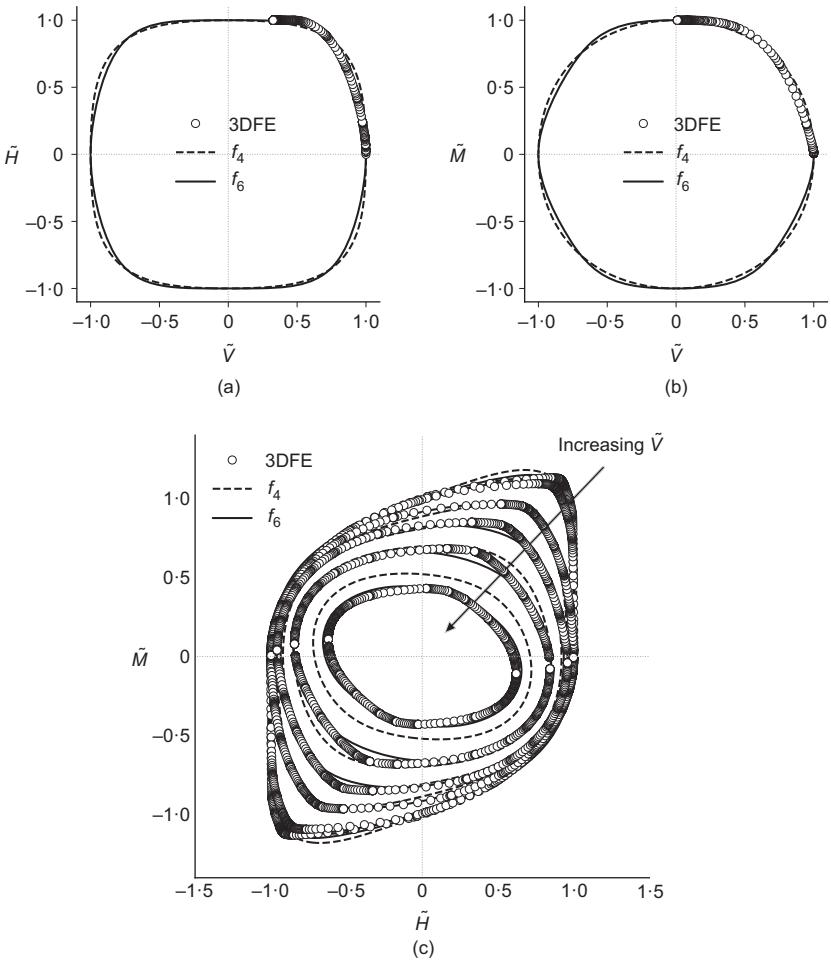

Fig. 2. Comparison of the normalised *VH*, *VM* and *HM* failure envelopes predicted by f_4 and f_6 with 3D finite-element (denoted 3DFE in figure) results (Suryasentana *et al.*, 2019) for a surface foundation. The *HM* envelopes correspond to normalised vertical loads: $\tilde{V}$ = 0, 0·25, 0·5, 0·625, 0·75, 0·875

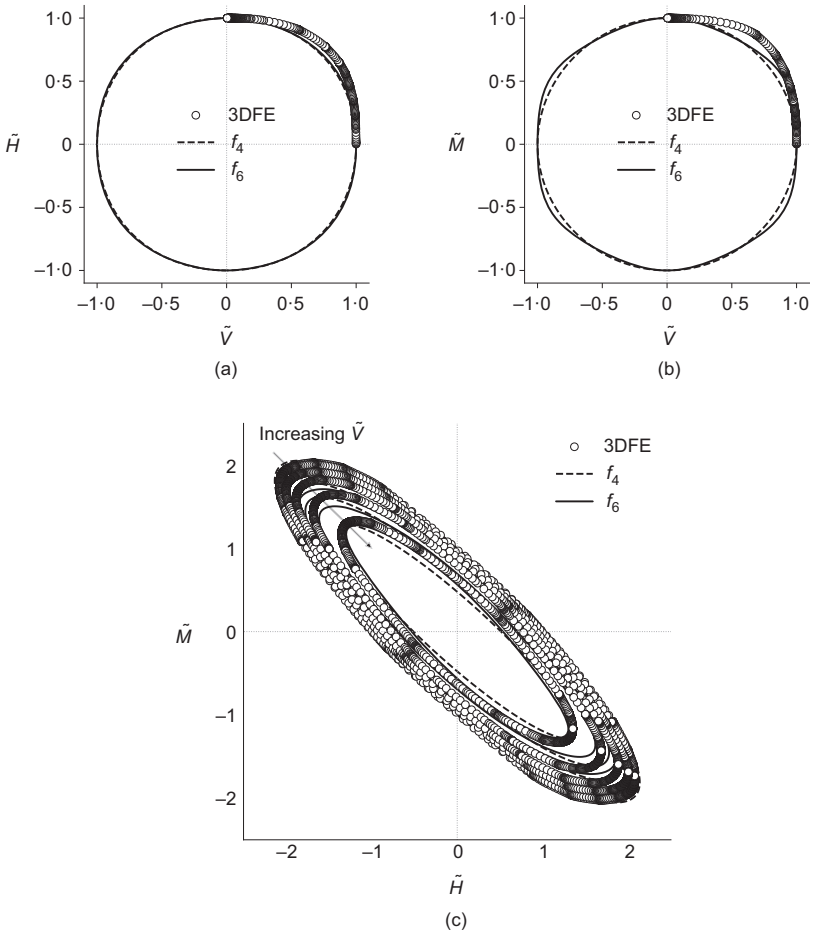

Fig. 3. Comparison of the normalised *VH*, *VM* and *HM* failure envelopes predicted by f_4 and f_6 with the 3D finite-element results (Suryasentana *et al.*, 2019) for a suction caisson foundation. The *HM* envelopes correspond to normalised vertical loads: $\tilde{V} = 0$, 0·25, 0·5, 0·625, 0·75, 0·875

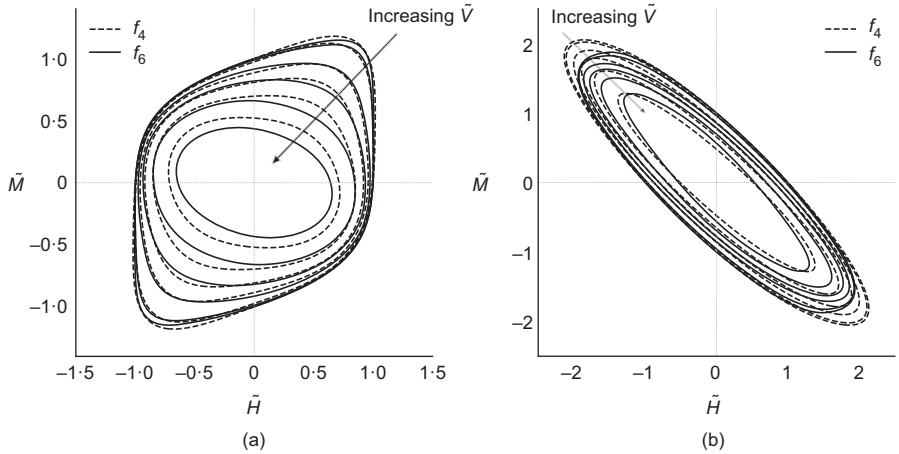

Fig. 4. Comparison of the normalised *HM* failure envelopes predicted by f_4 and f_6 under increasing vertical loading (i.e. $\tilde{V} = 0$, 0·25, 0·5, 0·625, 0·75, 0·875): (a) surface foundation; (b) suction caisson foundation

or, alternatively

$$f(\tilde{H}, \tilde{M}, \tilde{V}) = (\tilde{H}^2 + \tilde{M}^2 - 2e\tilde{H}\tilde{M})^{1/2\beta_2} - \tilde{\beta}^{1/\beta_2}\tilde{V}^{\beta_1/\beta_2}(1-\tilde{V}) = 0 \quad (15)$$

where $e = 0{\cdot}518 + 1{\cdot}18\tilde{V}(\tilde{V}-1)$, $\beta = (\beta_1+\beta_2)^{(\beta_1+\beta_2)}/\beta_1^{\beta_1}\beta_2^{\beta_2}$, and $\beta_1 = 0{\cdot}764$ and $\beta_2 = 0{\cdot}882$ are parameters, selected to fit the model to the data. It is instructive to use the new failure envelope framework to develop an alternative version

Table 3. Minimised objective values (and corresponding root-mean values) for f_4 and f_6 at the end of the optimisation process for the surface and caisson foundation results from Suryasentana *et al.* (2019)

Foundation	C for f_4	C for f_6	$\sqrt{C/n\text{data}}$ for f_4	$\sqrt{C/n\text{data}}$ for f_6
Surface	36·96	31·05	0·270	0·248
Caisson	20·3	20·35	0·246	0·247

Note: *n*data is the number of sets of failure load combinations (*n*data = 506 and *n*data = 335 for the surface and caisson foundation, respectively).

of Model B, to demonstrate how the new framework can be applied to existing formulations.

Failure envelope data were generated using equation (15) in the form of the $\tilde{V}\tilde{H}$ failure envelope, $\tilde{V}\tilde{M}$ failure envelope and the $\tilde{H}\tilde{M}$ failure envelopes for $\tilde{V} = 0{\cdot}125, 0{\cdot}25, 0{\cdot}375, 0{\cdot}5, 0{\cdot}625, 0{\cdot}75, 0{\cdot}875$. The data were standardised according to equation (8), where the adopted shift parameters were $[\tilde{H}_c, \tilde{M}_c, \tilde{V}_c] = [0, 0, 0{\cdot}5]$. Thus, $[\tilde{H}_{ref}, \tilde{M}_{ref}, \tilde{V}_{ref}] = [0{\cdot}995, 0{\cdot}995, 0{\cdot}5]$ (the failure envelope intersects the $\tilde{H}$ and $\tilde{M}$ axes at $\tilde{H} = \pm 0{\cdot}995$ and $\tilde{M} = \pm 0{\cdot}995$ when $\tilde{V} = \tilde{V}_c = 0{\cdot}5$, from equation (15)).

Failure envelopes have been determined on the basis of f_4 and f_6 (i.e. equations (12) and (13)) incorporating the same uniaxial and symmetry conditions as adopted in the earlier section 'Surface and caisson foundations' examples. The remaining coefficients were determined using the optimisation in equation (11).

Table 4. Best-fit coefficients in f_4 for the Model B failure envelope data

a_2	a_3	a_4	a_{10}	a_{11}	a_{12}
−0·86	2	−0·86	3·48	−2·93	3·48

The computed coefficients are listed in Tables 4 and 5. Fig. 5 shows the normalised VH, VM and HM failure envelopes for $f_4 - 1 = 0$ and $f_6 - 1 = 0$, together with comparisons with the original Model B equation. Evidently, both f_4 and f_6 provide reasonably good approximations of the Model B equation (although neither of them predicts the correct value of $\tilde{V}$ at which the peaks in the $\tilde{V}\tilde{H}$ and $\tilde{V}\tilde{M}$ envelopes occur). Table 6 shows the minimised objective function values (and their root-mean) for f_4 and f_6 at the end of the optimisation; these data suggest that f_4 provides a better fit than f_6. Figs 5(a) and 5(b) show that, at $\tilde{V} = 0$ and $\tilde{V} = 1$, the failure envelopes implied by f_4 and f_6 are more 'rounded' than Model B, and the surface normal is directed along the $\tilde{V}$ axis. This means that, when employed as a plastic potential, the model correctly predicts vertical plastic displacement for pure vertical loading; this is significant, as special numerical procedures are required to achieve such behaviour with Model B (Martin, 1994). In general, the results show that the SOS-convex Model B formulation provides a failure envelope that is reasonably close to the formulation in equation (15), although it is evident from Fig. 5(c) that the SOS-convex formulation is unconservative for relatively high values of normalised vertical load; the SOS-convex formulation, however, is guaranteed to be globally convex and well-behaved.

Table 5. Best-fit coefficients in f_6 for the Model B failure envelope data

a_2	a_3	a_4	a_5	a_6	a_{14}	a_{15}	a_{16}	a_{17}	a_{18}	a_{23}	a_{24}	a_{25}
−1·35	3·59	−2·74	3·59	−1·35	3·56	−4·94	8·94	−4·94	3·56	7·37	−6·59	7·37

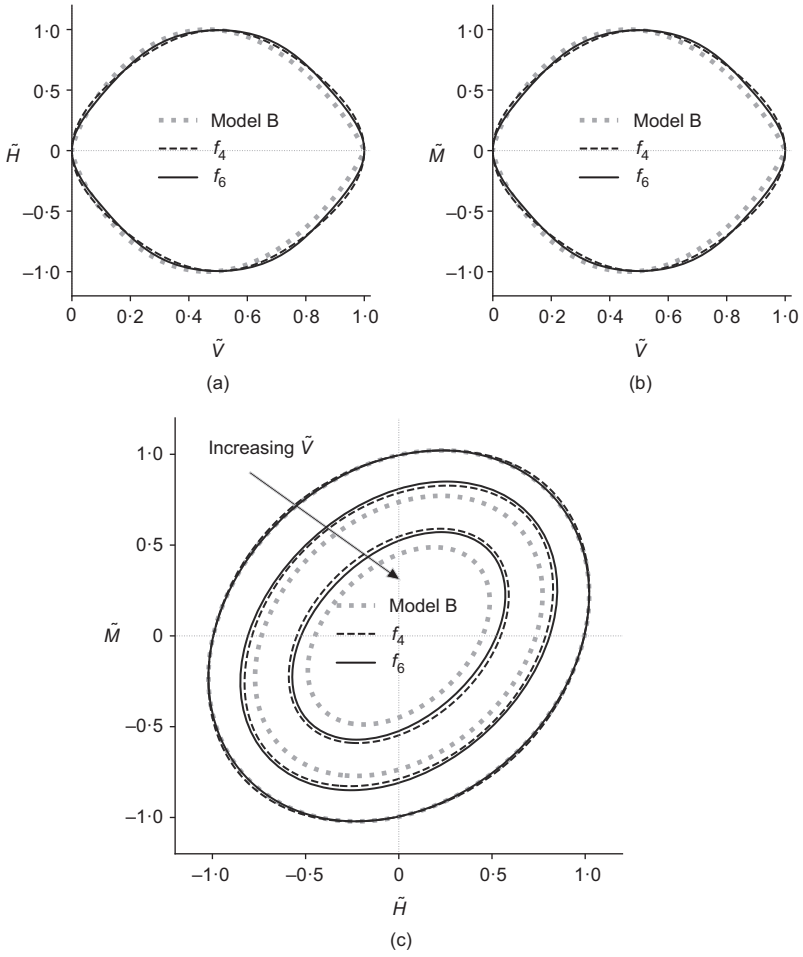

Fig. 5. Comparison of the normalised VH, VM and HM failure envelopes predicted by f_4 and f_6 with the original Model B equation. The HM envelopes correspond to normalised vertical loads: $\tilde{V} = 0{\cdot}5, 0{\cdot}75, 0{\cdot}875$

Macro-element model for a surface foundation

To demonstrate the application of the proposed SOS-convex failure envelope formulations in a macro-element model, the 4th degree version of the failure envelope (equation (12)) was employed, using the coefficients for a surface foundation in Table 1. Failure envelopes of the form $f(\tilde{H}, \tilde{M}, \tilde{V})$ such as equation (12) are implicit functions of the loading variables H, M, V by way of the affine transformation in equation (8) (in this case, $\tilde{H} = H/H_0$, $\tilde{M} = M/M_0$ and $\tilde{V} = V/V_0$). The failure envelope $f_4(H, M, V) - 1 = 0$ was implemented as the yield surface and plastic potential of a macro-element model, with the elasto-plastic integration performed using the implicit closest point projection method (Simo & Hughes, 2006). The uniaxial capacities (V_0, H_0, M_0) were determined from the finite-element data in Suryasentana *et al.* (2019), while the elastic stiffness matrix for the macro element was calibrated using pre-failure data obtained from the finite-element results.

Table 6. Minimised objective values (and corresponding root-mean values) for f_4 and f_6 at the end of the optimisation process for the Model B example

Foundation	C for f_4	C for f_6	$\sqrt{C/n\text{data}}$ for f_4	$\sqrt{C/n\text{data}}$ for f_6
Model B	8·23	11·22	0·0476	0·0556

Note: $n$data = 3634 is the number of sets of failure load combinations.

The macro-element model is used, as an example, to simulate a sequential swipe test in the HM load space for planar HM loading with $\tilde{V} = 0{\cdot}25$, to replicate the corresponding finite-element simulations in Suryasentana *et al.* (2019). Fig. 6 provides a comparison of the load–displacement behaviour and the normalised HM failure envelope, computed using the macro-element model and the 3D finite-element model (Suryasentana *et al.*, 2019). It is evident that the macro-element predictions agree well with the finite-element results.

DISCUSSION

The procedures presented in the paper provide a convenient means of generating failure envelopes that are convex and well-behaved. This is achieved by selecting functions from a restricted set of SOS-convex polynomials. The process is demonstrated by applying it to previously published numerical data on failure load combinations for a surface footing and a caisson on soil that is modelled as an elastic–perfectly plastic von Mises material. Additionally, it is used to reformulate a previously determined failure envelope, Model B.

The results indicate that an SOS-convex polynomial of degree 6, f_6, does not necessarily provide a better fit to a prescribed data set than an SOS-convex polynomial of degree 4, f_4. The results indicate that f_6 is a better fit for the surface foundation failure envelope than f_4, but the opposite is true for the caisson and Model B failure envelopes. This may seem counterintuitive, but it is a consequence of the fact that

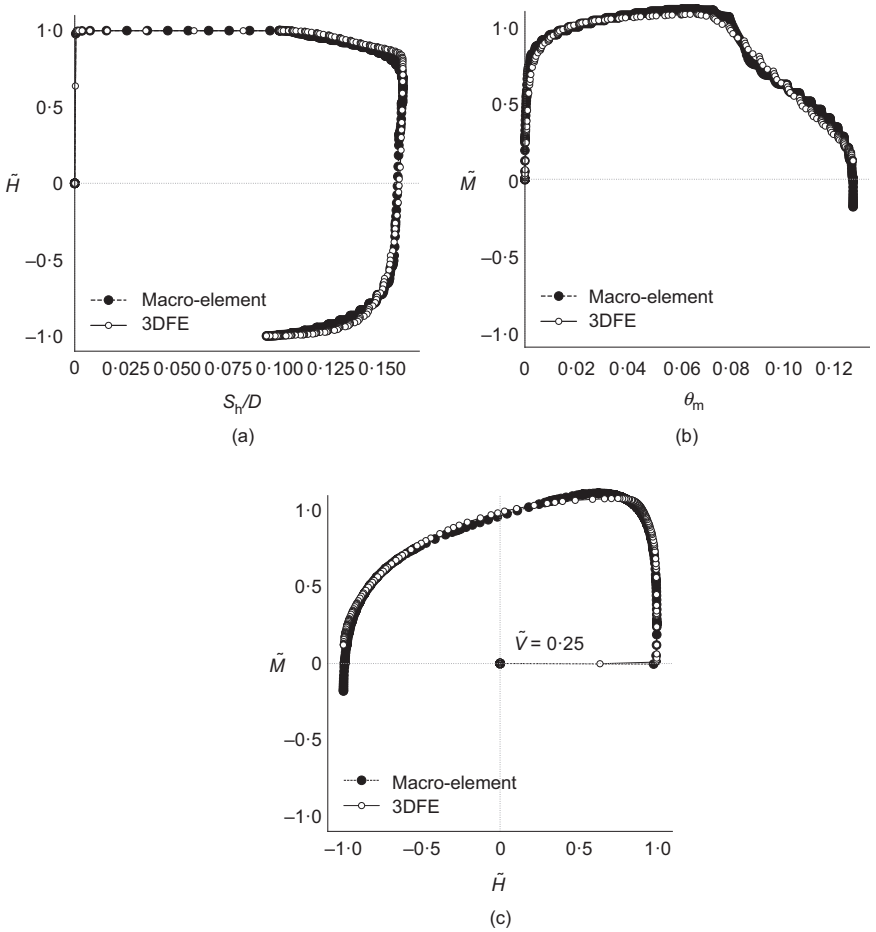

Fig. 6. Comparison of load–displacement and the normalised HM failure envelopes predicted by the macro-element and 3D finite-element results (Suryasentana *et al.*, 2019), for a sequential swipe test in the HM load space when $\tilde{V} = 0{\cdot}25$. S_h and θ_m refer to the horizontal and rotational displacements of the surface foundation, respectively. D is the diameter of the surface foundation

the current approach is restricted to the use of homogeneous polynomials. Although a general polynomial can be used to represent any polynomial of lower degree, this is not the case for the homogeneous polynomials employed here. For practical applications of this method, it is recommended that a relatively low degree homogeneous polynomial (e.g. degree = 4) is initially adopted. Higher degree polynomials would then be considered if the low degree polynomial is found to provide an unsatisfactory fit to the data.

The YALMIP toolbox provides a useful SOS decomposition feature to double check that the failure envelopes are, indeed, convex throughout the entire domain. For example, for f_4 employed for Model B, the Hessian can be decomposed into SOS form using YALMIP as

$$\begin{aligned}\bar{\boldsymbol{y}}^{\mathrm{T}}\nabla^2 f_4(\bar{\boldsymbol{x}})\bar{\boldsymbol{y}} = &\left(-3{\cdot}2835\bar{V}\bar{V}_1 - 3{\cdot}0493\bar{M}\bar{M}_1 + 0{\cdot}9486\bar{M}\bar{H}_1 + 0{\cdot}9486\bar{H}\bar{M}_1 - 3{\cdot}0493\bar{H}\bar{H}_1\right)^2 \\ &+ \left(-2{\cdot}0827\bar{V}\bar{M}_1 + 2{\cdot}0827\bar{V}\bar{H}_1 - 2{\cdot}0827\bar{M}\bar{V}_1 + 2{\cdot}0827\bar{H}\bar{V}_1\right)^2 \\ &+ \left(-1{\cdot}1788\bar{V}\bar{M}_1 - 1{\cdot}1788\bar{V}\bar{H}_1 - 1{\cdot}1788\bar{M}\bar{V}_1 - 1{\cdot}1788\bar{H}\bar{V}_1\right)^2 \\ &+ \left(-1{\cdot}5127\bar{M}\bar{M}_1 + 1{\cdot}5127\bar{H}\bar{H}_1\right)^2 + \left(-1{\cdot}3083\bar{M}\bar{H}_1 + 1{\cdot}3083\bar{H}\bar{M}_1\right)^2 \\ &+ \left(0{\cdot}0816\bar{V}\bar{V}_1 + 0{\cdot}3209\bar{M}\bar{M}_1 + 1{\cdot}1727\bar{M}\bar{H}_1 + 1{\cdot}1727\bar{H}\bar{M}_1 + 0{\cdot}3209\bar{H}\bar{H}_1\right)^2 \\ &+ \left(0{\cdot}7908\bar{V}\bar{M}_1 + 0{\cdot}7908\bar{V}\bar{H}_1 - 0{\cdot}7908\bar{M}\bar{V}_1 - 0{\cdot}7908\bar{H}\bar{V}_1\right)^2 \\ &+ \left(0{\cdot}7792\bar{V}\bar{M}_1 - 0{\cdot}7792\bar{V}\bar{H}_1 - 0{\cdot}7792\bar{M}\bar{V}_1 + 0{\cdot}7792\bar{H}\bar{V}_1\right)^2 \\ &+ \left(-1{\cdot}1009\bar{V}\bar{V}_1 + 0{\cdot}5572\bar{M}\bar{M}_1 - 0{\cdot}1142\bar{M}\bar{H}_1 - 0{\cdot}1142\bar{H}\bar{M}_1 + 0{\cdot}5572\bar{H}\bar{H}_1\right)^2\end{aligned} \tag{16}$$

where $\bar{\boldsymbol{x}} = [\bar{V}, \bar{H}, \bar{M}]^{\mathrm{T}}$, $\bar{\boldsymbol{y}} = [\bar{V}_1, \bar{H}_1, \bar{M}_1]^{\mathrm{T}} \in$ domain of f_4. This equation demonstrates that $\bar{\boldsymbol{y}}^{\mathrm{T}}\nabla^2 f_4(\bar{\boldsymbol{x}})\bar{\boldsymbol{y}}$ is SOS, hence $\bar{\boldsymbol{y}}^{\mathrm{T}}\nabla^2 f_4(\bar{\boldsymbol{x}})\bar{\boldsymbol{y}} \geq 0$ for its entire domain; f_4 is therefore shown to be SOS-convex.

The values of the coefficients in the failure envelope polynomials determined using the proposed framework do not necessarily have a physical interpretation. This disadvantage is outweighed by the new approach being able to represent a wide range of failure envelope shapes, while maintaining desirable theoretical attributes. A simple way to interpret the polynomial coefficients would be to view their (absolute) magnitudes as indicative of the strength of coupling between the respective loading components at failure.

The framework presented in the paper has certain limitations, as follows. The application of the SOS-convex failure envelope formulation to macro-element modelling has only been demonstrated for perfect plasticity with associated flow. Further work is needed to develop the modelling approach for the case of non-associated flow and hardening plasticity. Furthermore, the current study only explores the application of homogeneous polynomials. Non-homogeneous SOS-convex polynomials are not explored, but they potentially provide greater expressiveness than homogeneous SOS-convex polynomials (since homogeneous polynomials are subsets of non-homogeneous polynomials). However, based on initial analyses using non-homogeneous polynomials, the SeDuMi solver employed in the current work encountered convergence problems for some of the above examples; this contrasts with the homogeneous polynomials where convergence issues did not occur. Further work is needed to explore the implementation of non-homogeneous SOS-convex polynomials and their potential benefits.

CONCLUSIONS

This paper introduces a novel SOS-convex polynomial-based framework to systematically formulate failure envelopes that are suitable for use in both ultimate capacity calculations and macro-element modelling. The approach is applicable to failure envelope data sets of multiple loading dimensions, and it is demonstrated in the current paper for VHM loading. The principal advantage of the proposed framework is that it leads to formulations for failure envelope functions (and yield functions) that are guaranteed to be globally convex and well-behaved. As discussed in this paper, these attributes lead to significant advantages in terms of theoretical considerations as well as the numerical stability of macro-element models.

Examples are presented to demonstrate the application of the framework to three different shallow foundation cases, with significantly different failure envelope shapes. These examples demonstrate the expressiveness and general capabilities of the proposed framework. The framework rationalises and expedites the formulation of failure envelopes and therefore supports the development of the failure envelope approach for design applications.

Although not shown here, this framework may have potential uses in other fields of solid mechanics, such as determining convex yield functions from experimentally determined yield data for different materials.

ACKNOWLEDGEMENT

The first author would like to acknowledge the generous support of Ørsted Wind Power for funding his DPhil studentship at the University of Oxford.

APPENDIX

Convex functions

A function f is defined to be convex if its domain is a convex set and

$$f[\theta\boldsymbol{x} + (1-\theta)\boldsymbol{y}] \leq \theta f(\boldsymbol{x}) + (1-\theta) f(\boldsymbol{y}) \tag{17}$$

for all $\boldsymbol{x}, \boldsymbol{y} \in$domain of f and for $0 \leq \theta \leq 1$ (Boyd & Vandenberghe, 2004). Depending on the differentiability of f, there are two equivalent conditions to equation (17) that characterise the convexity of f.

If f is differentiable (i.e. its gradient $\nabla f(\boldsymbol{x})$ exists everywhere in its domain), f is convex if its domain is a convex set and

$$f(\boldsymbol{y}) \geq f(\boldsymbol{x}) + \nabla f(\boldsymbol{x})^{\mathrm{T}}(\boldsymbol{y} - \boldsymbol{x}) \tag{18}$$

for all $\boldsymbol{x}, \boldsymbol{y} \in$domain of f. Equation (18) is known as the first-order condition (Boyd & Vandenberghe, 2004).

If f is twice differentiable (i.e. its Hessian $\nabla^2 f(\boldsymbol{x})$ exists everywhere in its domain), f is convex if its domain is a convex set and $\nabla^2 f(\boldsymbol{x})$ is positive semi-definite everywhere in its domain – that is

$$\boldsymbol{y}^{\mathrm{T}}\nabla^2 f(\boldsymbol{x})\boldsymbol{y} \geq 0 \tag{19}$$

for all $\boldsymbol{x}$, $\boldsymbol{y} \in$ domain of f. This is known as the second-order condition (Boyd & Vandenberghe, 2004) and is the principal condition for assessing the convexity of functions in the current paper. One way to determine whether a matrix is positive semi-definite is to check whether all of its eigenvalues are non-negative everywhere in its domain.

An example of a twice differentiable, convex function is the von Mises yield function, where it can be shown that the eigenvalues of the Hessian are always non-negative. The Tresca yield function is convex according to the general condition in equation (17), but since it is not differentiable over its entire domain (e.g. at the 'corners') then the more restrictive first- and second-order conditions do not apply.

A yield surface should not be confused with a yield function. A yield surface is usually defined as the zero level set of a yield function $f(x)$ (i.e. $\{x|f(x) = 0\}$). A convex yield surface does not necessarily imply convexity of $f(x)$. Conversely, if $f(x)$ is convex, then the yield surface is necessarily convex. These conditions arise from convex analysis relating convex functions and their sublevel sets (Boyd & Vandenberghe, 2004), where a k-sublevel set is defined as $\{x|f(x) \leq k\}$. In continuum plasticity, the 0-sublevel set of a yield function typically represents the set of admissible stress states.

NOTATION

$\mathbf{A}$	positive definite matrix representing an ellipsoid in quadratic form
$\mathbf{B}$	positive semi-definite matrix representing coefficients of an SOS polynomial
$\boldsymbol{c}$	centre coordinates of an ellipsoid
D	diameter of surface foundation
d	positive integer representing half the degree of an SOS polynomial
g_j	polynomial components of an SOS polynomial
H	horizontal load
H_0	horizontal uniaxial capacity
$\bar{H}$	normalised horizontal load
$\tilde{H}$	standardised horizontal load
M	moment
M_0	moment uniaxial capacity
$\tilde{M}$	standardised moment load
$\bar{M}$	normalised moment load
n	number of loading dimensions
$\mathbf{Q}$	matrix from Cholesky decomposition of $\mathbf{B}$
$\mathbb{R}^n$	real coordinate space of n dimensions
S_h	horizontal displacement of surface foundation
s	SOS polynomial
V	vertical load
V_0	vertical uniaxial capacity
$\tilde{V}$	standardised vertical load
$\bar{V}$	normalised vertical load
x_i	load component
$x_{i,\mathrm{c}}$	shift parameter
$x_{i,\mathrm{ref}}$	reference load
$\boldsymbol{z}$	vector of monomials up to and including degree d
θ_m	rotational displacement of surface foundation

REFERENCES

Ahmadi, A. A. & Parrilo, P. A. (2012). A convex polynomial that is not SOS-convex. *Math. Program.* **135**, No. 1–2, 275–292.

Ahmadi, A. A., Olshevsky, A., Parrilo, P. A. & Tsitsiklis, J. N. (2013). NP-hardness of deciding convexity of quartic polynomials and related problems. *Math. Program.* **137**, No. 1–2, 453–476.

Bienen, B., Byrne, B. W., Houlsby, G. T. & Cassidy, M. J. (2006). Investigating six-degree-of freedom loading of shallow foundations on sand. *Géotechnique* **56**, No. 6, 367–379, https://doi.org/10.1680/geot.2006.56.6.367.

Bransby, M. F. & Randolph, M. F. (1998). Combined loading of skirted foundations. *Géotechnique* **48**, No. 5, 637–655, https://doi.org/10.1680/geot.1998.48.5.637.

Boyd, S. & Vandenberghe, L. (2004). *Convex optimization*. Cambridge, UK: Cambridge University Press.

Byrne, B. W. & Houlsby, G. T. (2001). Observations of footing behaviour on loose carbonate sands. *Géotechnique* **51**, No. 5, pp. 463–466, https://doi.org/10.1680/geot.2001.51.5.463.

Byrne, B. W. & Houlsby, G. T. (2005). Investigating six degree-of-freedom loading on shallow foundations. In *Frontiers in offshore geotechnics* (eds S. Gourvenec and M. Cassidy), pp. 477–482. Boca Raton, FL, USA: CRC Press.

Cassidy, M. J. (1999). *Non-linear analysis of jack-up structures subjected to random waves*. PhD thesis, University of Oxford, Oxford, UK.

Feng, X., Randolph, M. F., Gourvenec, S. & Wallerand, R. (2014). Design approach for rectangular mudmats under fully three-dimensional loading. *Géotechnique* **64**, No. 1, 51–63, https://doi.org/10.1680/geot.13.P.051.

Franchi, A., Genna, F. & Paterlini, F. (1990). Research note on quasi-convexity of the yield function and its relation to Drucker's postulate. *Int. J. Plasticity* **6**, No. 3, 369–375.

Gottardi, G. & Butterfield, R. (1993). On the bearing capacity of surface footings on sand under general planar loads. *Soils Found.* **33**, No. 3, 68–79.

Gottardi, G., Houlsby, G. T. & Butterfield, R. (1999). Plastic response of circular footings on sand under general planar loading. *Géotechnique* **49**, No. 4, 453–469, https://doi.org/10.1680/geot.1999.49.4.453.

Gourvenec, S. (2007). Failure envelopes for offshore shallow foundations under general loading. *Géotechnique* **57**, No. 9, 715–728, https://doi.org/10.1680/geot.2007.57.9.715.

Houlsby, G. T. & Byrne, B. W. (2001). Discussion: comparison of European bearing capacity calculation methods for shallow foundations. *Proc. Instn Civ. Engrs – Geotech. Engng* **149**, No. 1, 63–64, https://doi.org/10.1680/geng.2001.149.1.63.

Löfberg, J. (2004). YALMIP: a toolbox for modeling and optimization in MATLAB. In *Proceedings of 2004 IEEE international conference on robotics and automation, New Orleans, LA, USA*, pp. 284–289. New York, NY, USA: Institute of Electrical and Electronics Engineers.

Löfberg, J. (2009). Pre- and post-processing sum-of-squares programs in practice. *IEEE Trans. Autom. Control* **54**, No. 5, 1007–1011.

Martin, C. M. (1994). *Physical and numerical modelling of offshore foundations under combined loads*. PhD thesis, University of Oxford, Oxford, UK.

Martin, C. M. & Houlsby, G. T. (2000). Combined loading of spudcan foundations on clay: laboratory tests. *Géotechnique* **50**, No. 4, 325–338, https://doi.org/10.1680/geot.2000.50.4.325.

Martin, C. M. & Houlsby, G. T. (2001). Combined loading of spudcan foundations on clay: numerical modelling. *Géotechnique* **51**, No. 8, 687–699, https://doi.org/10.1680/geot.2001.51.8.687.

Meyerhof, G. G. (1951). The ultimate bearing capacity of foundations. *Géotechnique* **2**, No. 4, 301–332, https://doi.org/10.1680/geot.1951.2.4.301.

Nova, R. & Montrasio, L. (1991). Settlements of shallow foundations on sand. *Géotechnique* **41**, No. 2, 243–256, https://doi.org/10.1680/geot.1991.41.2.243.

Ottosen, N. S. & Ristinmaa, M. (2005). *The mechanics of constitutive modeling*. Kidlington, UK: Elsevier.

Panteghini, A. & Lagioia, R. (2014). A fully convex reformulation of the original Matsuoka–Nakai failure criterion and its implicit numerically efficient integration algorithm. *Int. J. Numer. Analyt. Methods Geomech.* **38**, No. 6, 593–614.

Panteghini, A. & Lagioia, R. (2018a). An approach for providing quasi-convexity to yield functions and a generalized implicit integration scheme for isotropic constitutive models based on 2 unknowns. *Int. J. Numer. Analyt. Methods Geomech.* **42**, No. 6, 829–855.

Panteghini, A. & Lagioia, R. (2018b). An extended modified Cam-Clay yield surface for arbitrary meridional and deviatoric shapes retaining full convexity and double homothety. *Géotechnique* **68**, No. 7, 590–601, https://doi.org/10.1680/jgeot.17.P.016.

Parrilo, P. A. (2003). Semidefinite programming relaxations for semialgebraic problems. *Math. Program.* **96**, No. 2, 293–320.

Shen, Z., Feng, X. & Gourvenec, S. (2016). Undrained capacity of surface foundations with zero-tension interface under planar V-H-M loading. *Comput. Geotech.* **73**, 47–57.

Shen, Z., Bie, S. & Guo, L. (2017). Undrained capacity of a surface circular foundation under fully three-dimensional loading. *Comput. Geotech.* **92**, 57–67.

Simo, J. C. & Hughes, T. J. (2006). *Computational inelasticity* (vol. 7). New York, NY, USA: Springer Science & Business Media.

Sloan, S. W. & Booker, J. R. (1986). Removal of singularities in Tresca and Mohr–Coulomb yield functions. *Communs Numer. Methods* **2**, No. 2, 173–179.

Sturm, J. F. (1999). Using SeDuMi 1.02, a MATLAB toolbox for optimization over symmetric cones. *Optimization Methods and Software* **11**, No. 1–4, 625–653.

Suryasentana, S. K., Dunne, H. P., Martin, C. M., Burd, H. J., Byrne, B. W. & Shonberg, A. (2019). Assessment of numerical procedures for determining shallow foundation failure envelopes. *Géotechnique* https://doi.org/10.1680/jgeot.18.P.055.

Taiebat, H. A. & Carter, J. P. (2000). Numerical studies of the bearing capacity of shallow foundations on cohesive soil subjected to combined loading. *Géotechnique* **50**, No. 4, 409–418, https://doi.org/10.1680/geot.2000.50.4.409.

Tan, F. (1990). *Centrifuge and theoretical modelling of conical footings on sand*. PhD thesis, University of Cambridge, Cambridge, UK.

Terzaghi, K. (1943). *Theoretical soil mechanics*. New York, NY, USA: John Wiley and Sons.

Vesić, A. (1973). Analysis of ultimate loads of shallow foundations. *J. Soil Mech. Found.* **99**, No. 1, 45–73.

Vulpe, C. (2015). Design method for the undrained capacity of skirted circular foundations under combined loading: effect of deformable soil plug. *Géotechnique* **65**, No. 8, 669–683, https://doi.org/10.1680/geot.14.P.200.

Vulpe, C., Gourvenec, S. & Power, M. (2014). A generalised failure envelope for undrained capacity of circular shallow foundations under general loading. *Géotechnique Lett.* **4**, No. 3, 187–196, https://doi.org/10.1680/geolett.14.00010.